CHAPTER 4

Results and Discussion

4.1 Process Optimization for Pectin and Chlorogenic Acid Extraction

According to the analysis by the Design-Expert program, all responses were able to be predicted by the three process parameters. All experimental results are shown in Table 4.1. The results of the analysis and the model of each response were summarized in Table 4.2. The table shows that all models were significant at *p*-value ≤ 0.05.

Table 4.1 Experimental results of pectin and chlorogenic acid extraction in different conditions

Treatment	Label	Pectin yield (%)	DE (%)	Chlorogenic acid (mg/100 mL)	Total phenolic compounds* (mg/100 mL)
1	(1)	1.91 ± 0.42	50.52 ± 0.35	51.14 ± 0.38	52.86 ± 0.09
2	a	1.63 ± 0.03	36.94 ± 0.12	30.50 ± 2.76	49.28 ± 0.18
3	b	3.77 ± 0.10	54.59 ± 1.61	90.50 ± 0.26	67.38 ± 0.90
4	ab	3.76 ± 0.07	39.71 ± 1.14	33.93 ± 1.25	55.50 ± 0.22
5	c	2.50 ± 0.09	58.50 ± 0.26	62.70 ± 2.24	59.09 ± 0.05
6	ac	1.90 ± 0.00	39.07 ± 2.08	30.46 ± 2.31	45.14 ± 0.67
7	bc	3.79 ± 0.03	60.65 ± 1.49	72.41 ± 1.99	72.78 ± 0.26
8	abc	7.99 ± 0.37	33.98 ± 0.69	32.77 ± 0.58	59.64 ± 0.44
9	CP1	2.25 ± 0.05	46.53 ± 0.25	24.65 ± 1.41	52.06 ± 0.22
10	CP2	1.95 ± 0.13	50.65 ± 0.38	19.21 ± 1.54	49.36 ± 0.13
11	CP3	2.16 ± 0.05	51.34 ± 0.25	18.06 ± 0.72	48.90 ± 0.48

* Gallic acid equivalent

Table 4.2 Mathematical models of responses from pectin and chlorogenic acid extraction

Coefficients in terms of standardized factors	Parameter (Y*)			
	$\frac{1}{\text{Pectin yield (\%)}}$	Degree of esterification (%)	Chlorogenic acids (mg/100mL)	Total phenolic compounds** (mg/100mL)
β_0	0.4	47.50	20.64	50.11
β_1	0.0098	-9.32	-18.64	-5.32
β_2	-0.14	0.49	6.85	6.12
β_3	-0.044	1.30	-	1.45
β_{12}	-0.044	-	-5.42	-
β_{13}	-	-2.20	-	-1.45
β_{23}	-	-	-	-
β_{22}	-	-	29.91	7.60
p-value***	0.0084	0.0013	0.0004	0.0019
p-lack of fits***	0.1544	0.4267	0.1842	0.2756
R^2	0.8672	0.9309	0.9542	0.9580

* $Y = \beta_0 + \beta_1 x_1 + \beta_2 x_2 + \beta_3 x_3 + \beta_{12} x_1 x_2 + \beta_{13} x_1 x_3 + \beta_{23} x_2 x_3 + \beta_{11} x_1^2 + \beta_{22} x_2^2 + \beta_{33} x_3^2 + \beta_{123} x_1 x_2 x_3$
when x_1 is acid concentration, x_2 is temperature and x_3 is time
** Gallic acid equivalent
*** a significant level of $\alpha = 0.05$

4.1.1 Effect of process parameters on pectin yield (Kungsuwan and Wiriyacharee, 2015)

In the study, pectin yield ranged from 1.63 to 7.99 percent. The maximum yield was achieved at acid concentration of 0.1 M, extracting temperature of 90°C and extraction time of 120 minutes which were at the highest level of all process parameters in this study. To improve adequacy of the model, the response Y_1 was inversely transformed into Y_1' where:

$$Y_1' = \frac{1}{Y_1} \quad [23]$$

After analysis, low p-value of the model (0.0084) demonstrated that developed model was significant. The high p-value of the lack of fit (0.1544) implied that the lack of fit was insignificant relative to pure error, thus the model could be used to predict the pectin yield. Moreover, coefficient of determination

(R^2) value of 0.8672 indicated that the model represented a well-correlated relationship between the responses and process variables.

Coefficients of the model illustrated that extracting temperature (β_2 = -0.14) was the main influence on the pectin yield followed by extracting time and acid concentration, respectively. The coefficient of extraction time (β_3 = -0.044) also showed a positive impact on the pectin yield. On the other hand, the yield of pectin decreased as acid concentration (β_1 = 0.0098) increased. However, the strong positive interaction effect between acid concentration and temperature (β_{12} = -0.044) suggested that the yield could be increased with higher acid concentration and higher temperature. This interaction is graphically illustrated in the Figure 4.1, where pectin yields rapidly increase at strong acid concentration and high extracting temperature region.

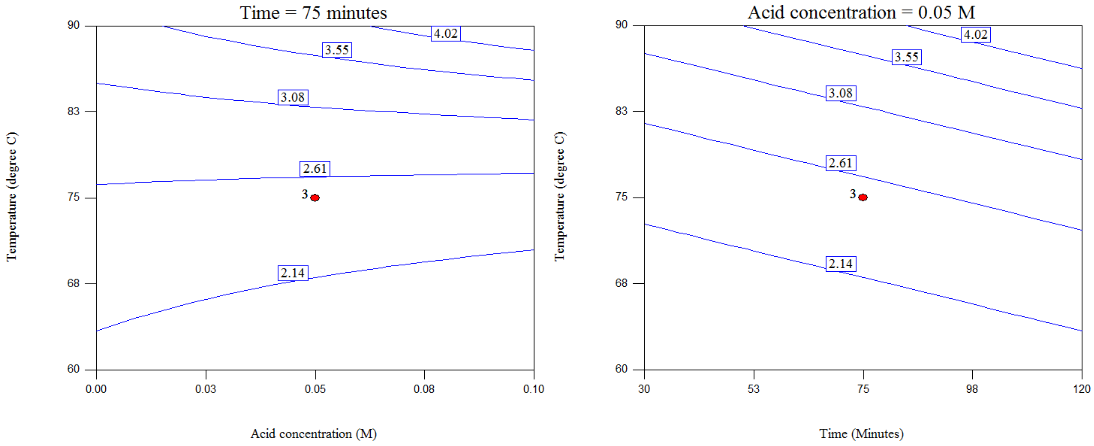

Figure 4.1 Effect of extraction parameters on pectin yield (%): Effect of acid concentration and temperature (left); Effect of time and temperature (right)

In this study, extracting temperature was the most significant parameter in determining pectin yield. Minjares-Fuentes *et al.* (2014) reported similar finding where the most influential parameter was extracting temperature. The study also suggested the significant positive effect on pectin yield when extraction time increased. However, the small negative effect from acid concentration in this study was contradicted the study from Minjares-Fuentes *et al.* (2014), which illustrated that the pectin yield gradually increased as acid concentration increased. This negative effect of acid concentration might come from a higher degree of pectin degradation as acid concentration increased (Mollea *et al.*, 2008). On the other hand, the strong synergistic effect between acid concentration and extracting temperature suggested that the yield of pectin could be improved with the use of higher extraction temperature coupled with stronger acid concentration. This effect was also observed by Wai *et al.* (2010) and Yeoh *et al.* (2008) from pectin extracted from durian rind and orange peel, respectively.

4.1.2 Effect of process parameters on pectin degree of esterification (Kungsuwan and Wiriyacharee, 2015)

By varying extracting condition, pectin from coffee pulp could be classified into both LMP and HMP. The minimum DE achieving from this experiment was 33.98 percent, while the maximum DE was 60.65 percent. The response model was significant with low *p*-value of 0.0013. The insignificant lack of fit and the high R^2 showed that the model could be used to predict the response.

With the value of -9.32, the highest coefficient in the model was β_1 indicated that acid concentration of extracting solution had the adverse effect on DE values. While the linear effect of extraction time (β_3 = 1.3) provided a positive impact to DE, its strong interaction with acid concentration (β_{13} = -2.2) would eventually overcome the impact resulted in a decrease in DE. Figure 4.2 clearly illustrates this alteration with a change in curvature of the contour plot. Finally, extracting temperature (β_2 = 0.49) had only a small effect to the DE of pectin, which was slightly increased as the temperature increased.

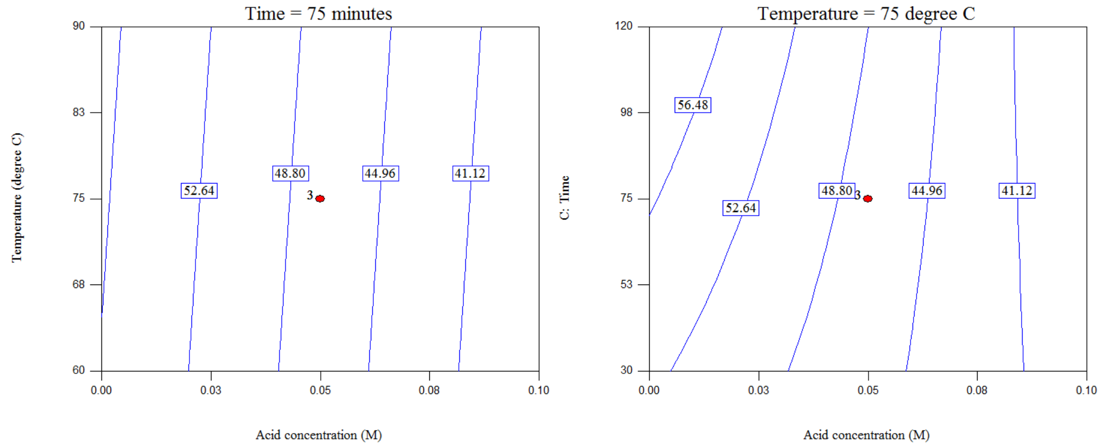

Figure 4.2 Effect of extraction parameters on pectin DE (%): Effect of acid concentration and temperature (left); Effect of acid concentration and time (right)

High negative effect of acid concentration and interaction between extraction time and acid concentration on pectin DE indicated that DE of pectin was greatly reduced by prolonging exposure to high concentration of acid. The same effect was observed by Wai *et al.* (2010), which claimed that the greatest effect on the DE of pectin obtained from durian rind was promoted by time and pH rather than temperature, because lower pH would increase a de-esterification of polygalacturonic chains (Mort *et al.*, 1993). Meanwhile, the small increase of DE from higher extracting temperature and higher extraction time might correspond to the higher yield of pectin which might slowly degrade.

4.1.3 Effect of process parameters on chlorogenic acid content (Kungsuwan and Wiriyacharee, 2015)

The yield of chlorogenic acid was in range of 18.06-90.50 mg/100 mL. In contrast to pectin yield, the treatment that yielded the highest amount of chlorogenic acid was achieved using no acid, extracting temperature of 90°C and 30 minutes of extraction time (Treatment 3). The model predicting chlorogenic acid content was significant with low *p*-value (0.0004), fit (lack of fit *p*-value = 0.1842) and well-correlated (R^2 = 0.9542).

Figure 4.3 shows the effect of acid concentration and extracting temperature on amount of chlorogenic acids. Unlike pectin yield and DE, chlorogenic acid content was not affected by extraction time. The extracting temperature (β_2 = 6.85

and β_{22} = 29.91) was the main influence showing parabolic relationship with the response which increased as the temperature deviated from the vertex of the parabola to 60°C or 90°C. On the contrary, the increase in acid concentration (β_1 = -18.64) would greatly decrease the yield of chlorogenic acids. The model also showed that there was a small interaction between acid concentration and extracting temperature which reduced the chlorogenic acid content in the extract as the interaction increase.

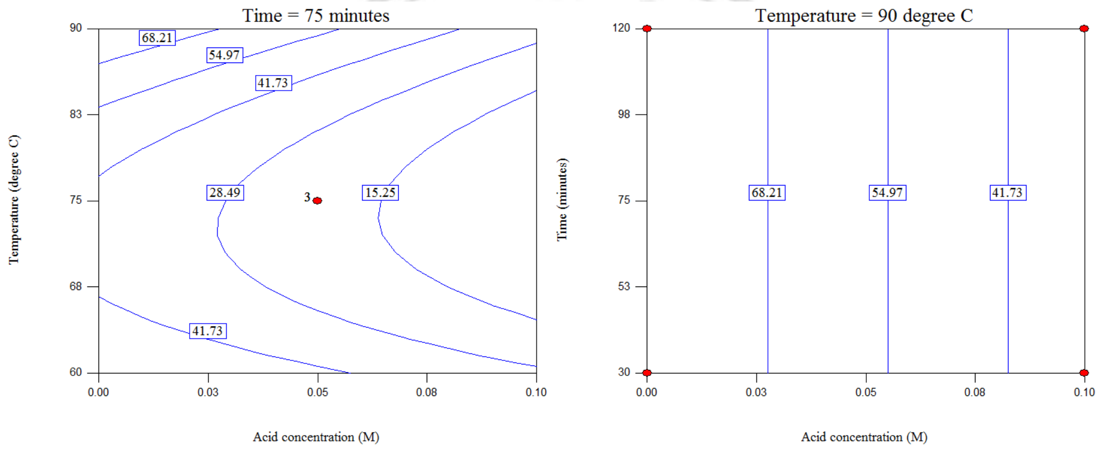

Figure 4.3 Effect of extraction parameter on chlorogenic acid content (mg/100 mL): Effect of acid concentration and temperature (left); Effect of acid concentration and time (right)

This study showed that the main variables affecting the yield of chlorogenic acids were extracting temperature and acid concentration. Acid concentration negatively affected the yield by degrading chlorogenic acid (Monsanto *et al.*, 2014). The effect was also seen in the research by Li *et al.* (2011) that yield chlorogenic acids extracted from sweet potato leave started to decrease when the pH decreased from 5 to 3. In contrast, an increase in temperature enhanced the yield of chlorogenic acid in a parabolic relationship where the yield abruptly increased when extracting temperature reaching 60°C or 90°C. Mazvimba *et al.* (2012) and Zhang *et al.* (2008) reported the optimum temperature for extracting chlorogenic acids was 70°C and 60°C, respectively. Therefore, the extractable chlorogenic acid content might already reach its maximum amount at the extracting temperature of 60°C. The increase in extracting temperature from that point onward would result in a loss of stability of chlorogenic acids, which reflected in the sudden loss of the yield after 60°C (Upadhyay *et al.*, 2012). On the other hand, the increase of chlorogenic acids near extracting temperature of 90°C could come from the degradation of plant cell walls which increased the amount of extractable chlorogenic acids (Padayachee *et al.*, 2012b). As a result, the more damage was done to the coffee pulp cell walls, the higher the yield of chlorogenic acids would be. This effect was also reflected by the great increase in pectin yield when the temperature reaching 90°C.

4.1.4 Effect of process parameters on total phenolic compounds

Total phenolic compounds behaved similarly with chlorogenic acid content, which the highest amount was achieved at extraction temperature of 90°C, 30 minutes of extraction time and without acid. The value was in between 45.14 and 67.38 mg gallic acid/100 mL. The mathematical model representing the response was significant, fit and well-correlated as well.

The most significant factor of this response was temperature (β_{22} = 7.6 and β_2 = 6.12), which affected the steady increase in total phenolic compounds as the temperature increased; as well as, the sudden increase of the yield as the temperature approaching 60 or 90°C. Another importance factor was acid concentration (β_2 = -5.32) that degraded phenolic compounds as the stronger acid was used. For extraction time, an increase in the parameter affected the increase in total phenolic compounds (β_3 = 1.45); but, the reverse effect was also observed when the extraction was performed with stronger acid concentration (β_{13} = -1.45). The overall effect of process parameters on total phenolic compounds is illustrated in Figure 4.4.

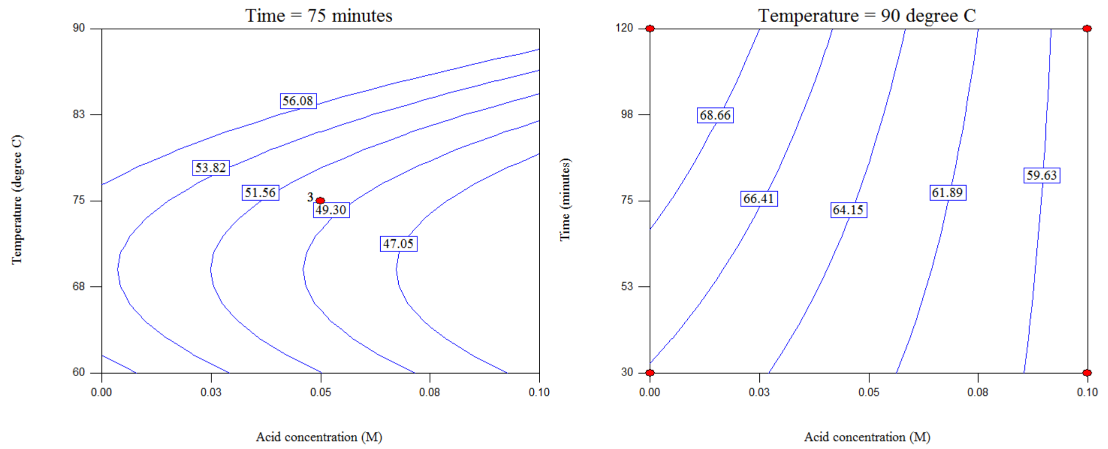

Figure 4.4 Effect of extraction parameter on total phenolic compounds (mg gallic acid equivalent/mL): Effect of acid concentration and temperature (left); Effect of acid concentration and time (right)

As the two major classes of polyphenols in coffee pulp are chlorogenic acids and anthocyanin (Ramirez-Coronel *et al.*, 2004), the response of the total phenolic compounds would follow the behavior of both compounds. Both compounds are membrane-bound polyphenols (Padayachee *et al.*, 2012a, 2012b). The bounding caused the parabolic response of total phenolic compounds with varying temperature. For instance, the high yield at 60°C resulted from the molecules that already unbounded; while, the increase in the yield when temperature approaching 90°C was the result of destroyed cell wall releasing the compounds. In contrast, the increase in acid concentration degraded both compounds (Li *et al.*, 2011; Li *et al.*, 2013). But the effect of temperature and acid concentration was less pronounced than that of chlorogenic acid content, which is the major constituent of phenolic compounds in coffee pulps; thus, the response should behave the same way. The reason for this is that there is other polyphenols in the extract that are stable in strong thermic and acidic conditions. The compounds are most likely be tannins that stable in those conditions as mentioned by Parisi *et al.* (2014). Hence, the presence of tannins resulted in less influence of process parameters on total phenolic compounds.

4.1.5 Optimization

Figure 4.5 shows the optimum point where the highest yield of pectin, chlorogenic acids and phenolic compounds were achieved with pectin DE less than 50% (so that the pectin is LMP). The optimum condition in extracting pectin and chlorogenic acids was using 0.04 M HCl concentration as extracting solvent at 90°C for 60 minutes. The resulting extract contained chlorogenic acids at an amount of 62.21 mg per 100 mL, total phenolic compounds at the amount of 64.31 mg gallic acid equivalent per 100 mL; and, had pectin yield of 3.58% with DE of 49.27% (predicted values).

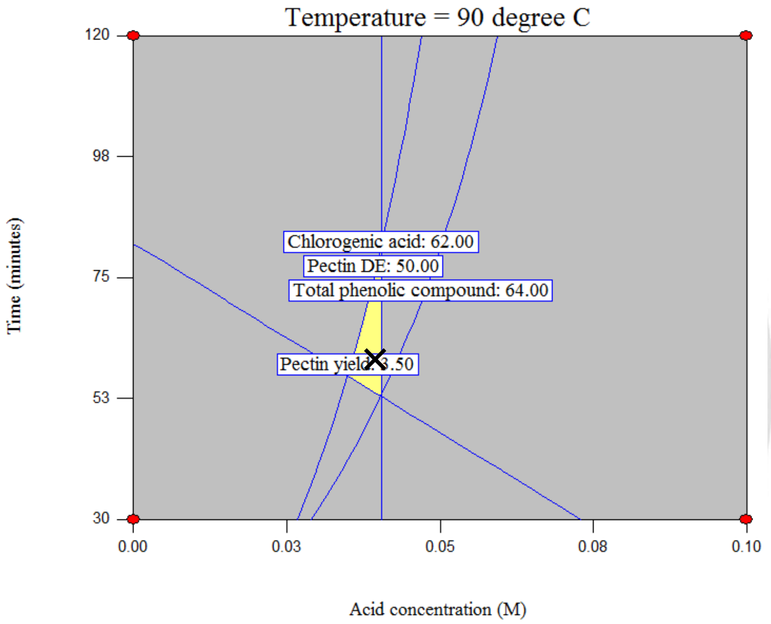

Figure 4.5 Graphical optimization of extraction condition (✕ = optimum point)

As suspected, the chlorogenic acid content in the extract and pectin yield reacted differently to extraction parameters. For instance, if the acid concentration was increased along with extraction time and temperature, the yield of pectin would greatly increase. In contrast, the amount of chlorogenic acid in the resulting extract would significantly reduce due to the degradation.

Nonetheless, the research showed that high amount of chlorogenic acids could be attained at high temperature. This advantage allowed the extraction process of both pectin and chlorogenic acids to be performed simultaneously in one process. Though, the maximum yield of one compound could not be achieved without compromising another, the benefit in cost and time reduction for extracting the two compounds together was worthwhile.

4.2 Process Optimization for CMC Synthesis

Table 4.3 summarizes CMC yield and DS of CMC from all treatments. Based on the results, the mathematical models representing CMC yield and DS in term of NaOH concentration were evaluated and summarized in Table 4.4. All models were significant with *p*-values less than 0.05, fit (*p*-lack of fit > 0.05) and well-correlated ($R^2 > 0.9$)

Table 4.3 Experimental results of CMC synthesis in different NaOH concentration

Treatment	NaOH concentration (g/100 mL)	Yield (%)	Degree of substitution
1	20	110.00	0.5494 ± 0.0065
2	30	166.73	0.9107 ± 0.0200
3	40	154.67	1.0104 ± 0.0302
4	50	109.80	0.7313 ± 0.0029
5	60	101.73	0.4032 ± 0.0194
6	30	156.67	0.9507 ± 0.0616
7	50	111.60	0.7617 ± 0.0015

Table 4.4 Mathematical models of responses from CMC synthesis

Coefficients in terms of standardized factors	Parameter (Y*)	
	Yield (%)	Degree of substitution
β_0	149.1	0.98
β_1	-66.62	-0.11
β_{11}	-44.16	-0.51
β_{111}	62.49	-
p-value**	0.0053	0.0015
p-lack of fits**	0.3136	0.1122
R^2	0.9786	0.9618

* $Y = \beta_0 + \beta_1 x + \beta_{11} x^2 + \beta_{111} x^3$ where x is a NaOH concentration
** a significant level of $\alpha = 0.05$

4.2.1 Effect of NaOH concentration on CMC yield

CMC yields were over 100% due to substitution of higher molecular weight carboxymethyl groups with hydroxyl groups. Figure 4.6 shows the effect of

NaOH concentration on the yield of CMC. Yield of CMC was increased as NaOH concentration increased until it reached a maximum point. The predicted maximum yield of CMC of 164.68% was achieved using 31.89% NaOH concentration. After that point, the yield was gradually dropped as the concentration increased. The increase in CMC yield during the first period of increasing NaOH concentration is the result NaOH expanding the molecules of CMC, which increased the reaction sites (Equation [1]). More reaction sites promoted the etherification process (Equation [2]) resulting in higher yield. But, when all accessible reaction sites were expanded, addition of NaOH would promote the side reaction that produced sodium glycolate (Equation [3]) instead of CMC. As a result, CMC yield was decreased as the NaOH concentration was increased from the optimum point (Pushpamalar *et al.*, 2006; Rachtanapun *et al.*, 2012).

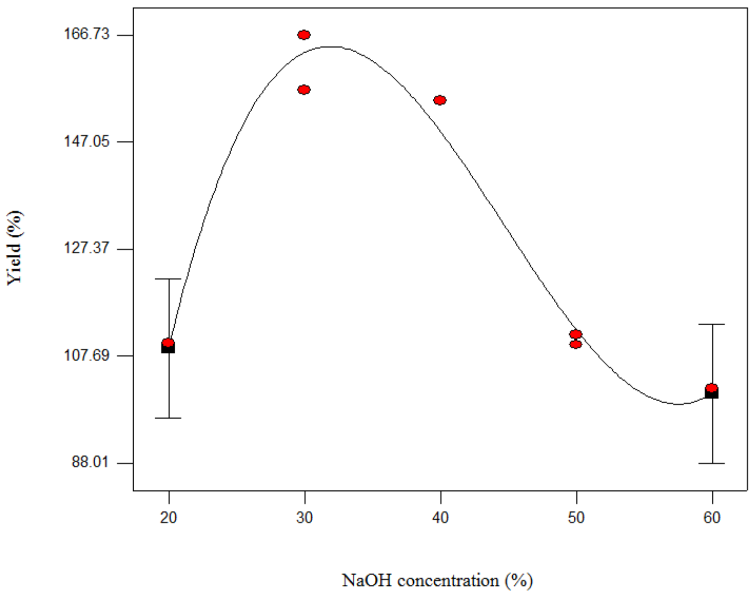

Figure 4.6 Effect of NaOH concentrations on CMC yield

4.2.2 Effect of NaOH concentration of DS

Degree of substitution (DS) measures how much of hydroxyl groups in the cellulose molecules are substituted by carboxymethyl groups. The higher the DS means the more substitution has occurred and the resulting CMC is more soluble. Similar to CMC yield, DS was increased as the NaOH concentration increased until it reached optimum concentration (Figure 4.7). The optimum NaOH concentration was at 37.83% with predicted DS of 0.9824. Correspondingly, the reason for the increase in DS was the increasing NaOH that partially modified cellulose molecule and made it ready for the substitution. The more NaOH was increased, the more hydroxyl groups of cellulose were exposed to the monochloroacetate. But, further increase in NaOH concentration from the optimum point would result in the side reaction of sodium glycolate and reduce the DS of CMC (Pushpamalar *et al.*, 2006; Rachtanapun *et al.*, 2012).

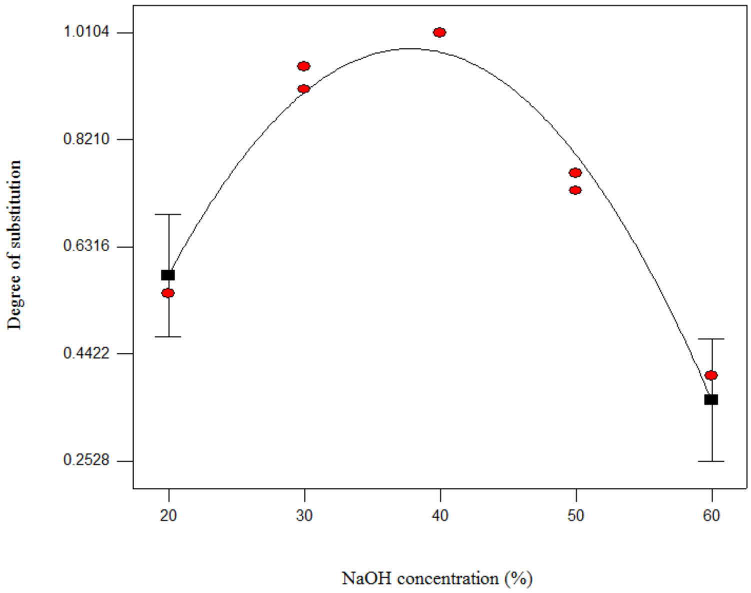

Figure 4.7 Effect of NaOH concentrations on DS

4.2.3 Optimization

In this experiment, there was a slight variation between optimum NaOH concentrations from CMC yield and DS. Therefore, to obtain the optimum condition maximizing both responses, the numerical optimization using Design-Expert software was used. The optimum concentration was obtained based on the desirability. Figure 4.8 shows the desirability of various NaOH concentrations. The highest desirability is achieved at 33.88% NaOH concentration. For simplicity of processing, the chosen optimum NaOH concentration for synthesis of CMC was 34% NaOH concentration. The resulting yield and DS were predicted as 163.42% and 0.9639, respectively. The reason for the variation might come from measurement error or the impurity during the synthesis that might altered DS values of the samples.

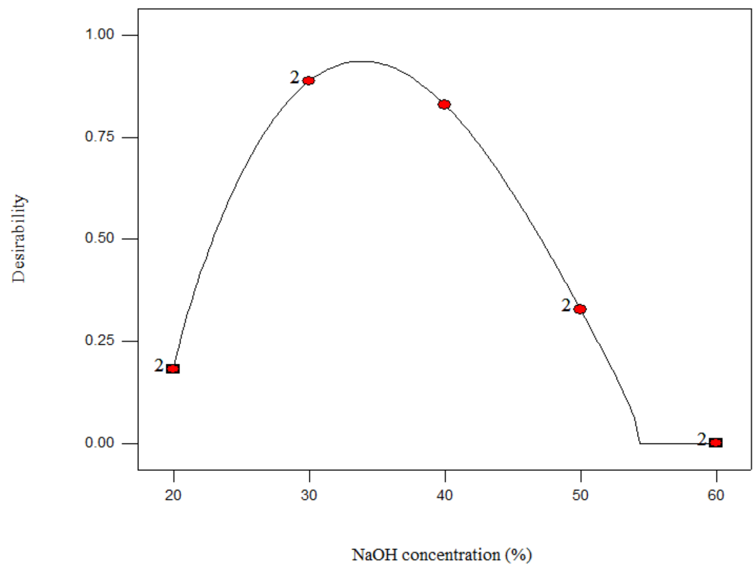

Figure 4.8 Desirability plot against various NaOH concentrations

4.3 Optimization of Film Formulation

The analysis of various film formulations was summarized in Table 4.5. Mathematical models of the responses were analyzed by Design-Expert software and the results were shown in Table 4.6. All models were significant with *p*-value less than 0.05. The responses were all well-correlated with the variables (R^2 > 0.90) and fit (*p*-lack of fit > 0.05).

Table 4.5 Experiment results of various film formulations

Formulation	CMC (%)	Chitosan (%)	Glycerol (%)	Thickness (mm)	Elongation (%)	Tensile Strength (MPa)	WVT ($g.h^{-1}.m^2$)
1	80	0	20	0.1596 ± 0.0096	131.12 ± 4.83	0.3858 ± 0.0025	0.9003 ± 0.0119
2	60	20	20	0.2322 ± 0.0142	26.21 ± 2.16	0.5669 ± 0.0063	0.9025 ± 0.1011
3	60	0	40	0.1608 ± 0.0215	74.50 ± 10.58	0.0375 ± 0.0006	1.1316 ± 0.1253
4	70	10	20	0.2113 ± 0.0080	52.57 ± 2.60	0.7393 ± 0.0039	0.5800 ± 0.1401
5	70	0	30	0.1445 ± 0.0167	72.28 ± 16.39	0.0360 ± 0.0006	1.1182 ± 0.0394
6	60	10	30	0.2157 ± 0.0215	44.43 ± 2.16	0.3897 ± 0.0039	0.9930 ± 0.0137
7	66.67	6.67	26.67	0.1802 ± 0.0118	58.91 ± 2.91	0.5117 ± 0.0041	0.8400 ± 0.0422
8	66.67	6.67	26.67	0.1727 ± 0.0103	53.79 ± 5.31	0.4112 ± 0.0036	0.8589 ± 0.1021
9	66.67	6.67	26.67	0.1833 ± 0.0066	58.52 ± 7.89	0.4177 ± 0.0029	0.8840 ± 0.1101

Table 4.6 Mathematical models of responses from film formulation

Coefficients in term of pseudo component	Parameter (Y*)		
	Elongation (%)	Tensile Strength (MPa)	Permeance (g.h-1.m2)
β_1	130.33	0.320	0.90
β_2	24.76	0.610	0.89
β_3	73.06	0.016	1.12
β_{12}	-87.22	1.130	-1.31
β_{13}	-104.97	-	0.38
β_{23}	-	-	-
p-value**	0.0004	0.0044	0.0002
p-lack of fits**	0.2077	0.2488	0.5448
R^2	0.9885	0.913	0.9918

* $Y = \beta_1 x_1 + \beta_2 x_2 + \beta_3 x_3 + \beta_{12} x_1 x_2 + \beta_{13} x_1 x_3 + \beta_{23} x_2 x_3 + \beta_{123} x_1 x_2 x_3$
where x_1, x_2 and x_3 is percent of CMC, chitosan and glycerol, respectively
** a significant level of $\alpha = 0.05$

4.3.1 Effect of film formulation on elongation at break

Elongation at break measures length of film that can be extended before break. In this study, coffee pulp films could be stretched from 26.21% to 131.12% of the original length. Figure 4.9 shows the effect of film composition on the response. CMC content (β_1 = 130.33) in the film was the most influential component in determining film elongation. The more CMC content, the longer the film was stretched. Secondly, increasing in glycerol (β_3 = 73.06), as a plasticizer, showed the strong effect of increasing the elongation as well. But, the increase of glycerol along with CMC (β_{13} = -104.97), would reduce the elongation of the film instead. The reduction was due to the film becoming too soft; thus, easily broken. The increasing chitosan content (β_2 = 24.76) in the film also showed the increasing effect on film elongation. However, the generation of polyelectrolyte complex from adding chitosan (β_{12} = -87.22) predominantly affected the film to be less elongated.

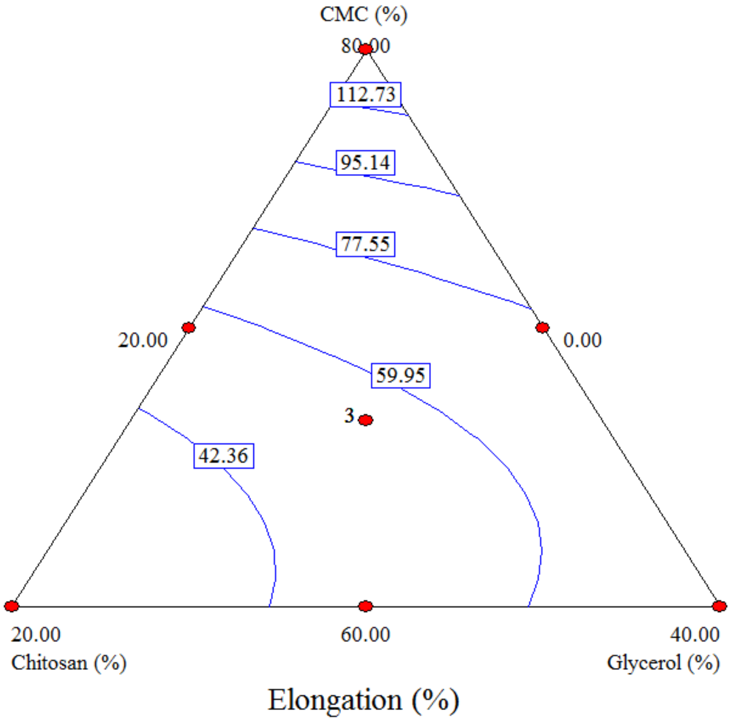

Figure 4.9 Effect of film formulation on elongation at break

Addition of plasticizer is well-known to increase the flexibility of the film, which can elongate more. Nonetheless, too much plasticizer in the film is likely to impede the intermolecular force of polymer; thus, the film can no longer be formed or become less cohesive. The adverse effect to elongation by adding glycerol to the film with high content of CMC in this study was similar with the study from Phuong and Lazzeri (2012). The study showed that the addition of excessive amount of plasticizer caused the film to be hampered in mechanical properties.

The less elongation from increasing chitosan content was the result of formed polyelectrolyte complex structure. Hence, addition of chitosan to the film formulation means addition the reinforcing agent into the film system. In this case, polyelectrolyte complex from chitosan, CMC and pectin, are in the form of tiny particles (see SEM micrographs in the following section). The presence of the complex acted like the composite of microstructures where the particles using the interacting forces between matrix and reinforcing agent to strengthen the film structure. But, the structure would impede the movement between polymer molecules; thus decrease its flexibility (Chen *et al.*, 2010).

4.3.2 Effect of film formulation of tensile strength

Figure 4.10 shows the tensile strength increases as both CMC (β_1 = 0.32) and chitosan contents (β_2 = 0.61) increase. In fact, the film became stronger as the interaction (β_{12} = 1.13) between those two was increased. The increase in glycerol means the reduction of both compounds, so it decreased the tensile strength of the film. Tensile strengths measured in this study were ranged from 0.0360 to 0.7393 MPa.

Improvement of tensile strength was mainly come from the present of polyelectrolyte complex structure as reinforcing agent in the matrix. Interaction in the interface caused the material to become stronger (Liu *et al.*, 2010). Moreover, ionic interaction between opposite charges of both polymers provided compatibility of the structure to the film as suggested by Chen *et al.* (2010). They stated that opposing charges in polymer system are bonding sites between polymers; thus, increase compatibility of the mixture and improve the strength of the film more than the film from single type of polymer can achieve. However, addition of chitosan content approximately more than 10% to the film formulation decreased tensile strength of the film. The reduction was caused by polyelectrolyte complex that coagulated when increased in concentration, which made the film to become brittle (Savadekar and Mhaske, 2012).

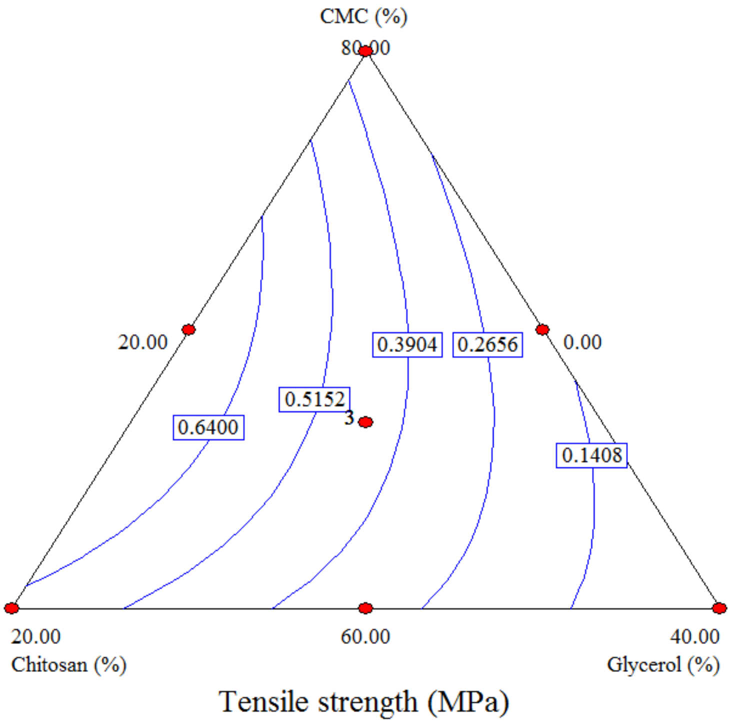

Figure 4.10 Effect of film formulation on tensile strength

4.3.3 Effect of film formulation on WVT

Coffee pulp film exhibited WVT from 0.5800 to 1.1316 $g.h^{-1}.m^{2}$. The most significant parameter that affected WVT of the film was interaction between CMC and chitosan content (β_{12} = -1.31) as the interaction increased the WVT decreased. Next was an amount of glycerol (β_3 = 1.12). The more glycerol content, the more WVT would be. An increase in CMC (β_1 = 0.89) and chitosan (β_2 = 0.90) content increased WVT as well. In addition, when the amount of CMC and glycerol were increased together (β_{13} = 0.38), WVT of the film was substantially increased.

Figure 4.11 shows an overall trend of WVT as the film formulation was varied. As suspected, the increase in glycerol resulted in the increase of WVT. Glycerol acts as plasticizer to films; thus, the increase in WVT can be attributed to the high affinity of glycerol to water which promotes the diffusion of water molecules (Laohakunjit and Noomhorm, 2004). Hydrophilicity of CMC and chitosan also contributed to the increase on WVT in this regards. But, the interaction of both compounds, which represented the formation of polyelectrolyte complex structure, impeded the transfer of water molecules. This phenomenon could be explained by the strong ionic interaction of the complex that decreased the thickness of the film (according to SEM micrograph in the next section). The increased film density with the presence of the polyelectrolyte complex would prevent the diffusion of water molecules through the film as explained by Silva *et al.* (2008).

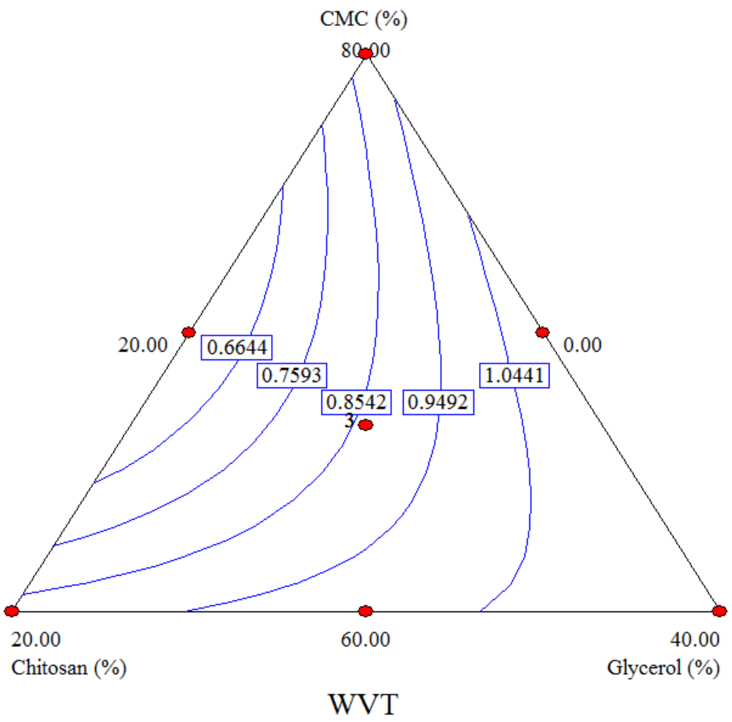

Figure 4.11 Effect of film formulation on WVT ($g.h^{-1}.m^2$)

4.3.4 Optimization

The film was optimized toward the strongest film with highest resistance to water and moderate elongation (more than 50%). Figure 4.12 illustrates the chosen optimum formulation of the most desirable film. The film showed a strongest tensile strength of 0.7474 MPa and lowest WVT of 0.5694 $g.h^{-1}.m^2$ while retain appropriate elongation at break at 55.74% (predicted values). The composition of the film included 70% CMC, 10% chitosan and 20% glycerol. Tenth percent had shown to be the most suitable amount of chitosan for the coffee pulp film which supported the hypothesis that effective structure of polyelectrolyte complex film could be formed by adding a minor amount of one polymer on top of existing network of another (Farris *et al.*, 2011). The less chitosan in the film would result in the weaker film due to lack of polyelectrolyte complex structure. But the more amount of chitosan in the film would likely to cause charge imbalance that would affect the stability of the structure. The unstable polyelectrolyte complex would agglomerate and form bigger particles; thus, more brittle film was resulted (Farris *et al.*, 2009).

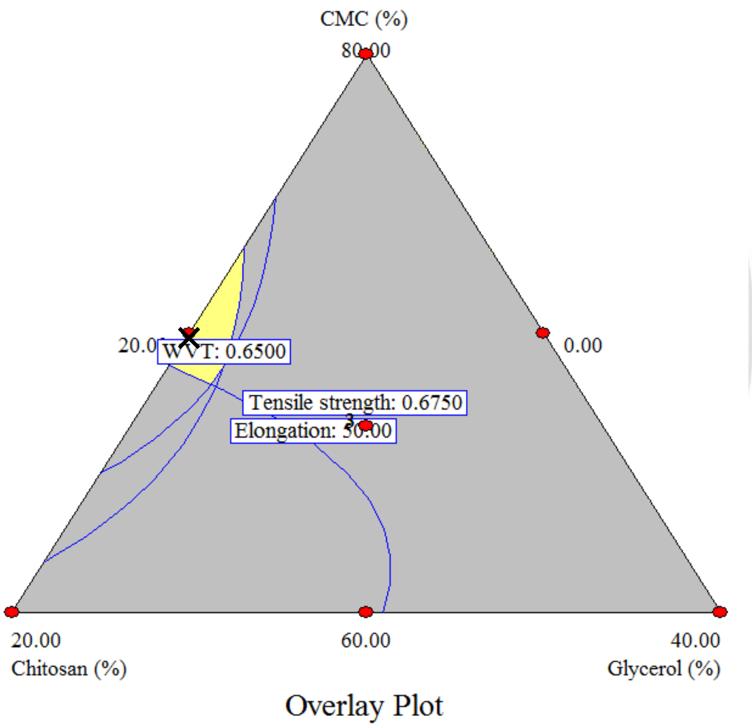

Figure 4.12 Graphical optimization of film formulation (× = optimum point)

When included the pectin, chlorogenic acid content and other components to the film formulation, the corrected final film formulation is summarized in Table 4.7.

Table 4.7 Corrected final film formulation

Film composition	%
CMC	53.61
Chitosan	7.66
Glycerol	12.25
Pectin	3.43
Chlorogenic acids	0.95
Hydrochloric acid	2.98
Acetic acid	10.21
Sodium chloride	10.21

4.4 Film Studies

Effects of polyelectrolyte complex on mechanical properties and water resistance are shown in Table 4.8. The film with polyelectrolyte complex (CC) showed double in tensile strength, half the rate of water transmission but less flexible when compared with the film without one (CM). The effect came from the polyelectrolyte complex structure reinforcing the film, which explained in section 4.3. Moreover, film with polyelectrolyte complex structure showed less solubility in water comparing to a full solubility of the film without polyelectrolyte complex structure. However, the polyelectrolyte film could retain more water as shown by higher moisture content. These effects might come from the structure of the polyelectrolyte complex that resembles hydrogel structure. The structure can sustain water while maintain its structural integrity (Farris *et al.*, 2009). Meanwhile, contact angle of the film showed that the film with polyelectrolyte complex structure had less hydrophilic surface than the film without polyelectrolyte complex, which was in contrast with the pectin-chitosan film studied by Chen *et al.* (2010). The study indicated that the addition of polyelectrolyte complex to the chitosan film increased the film hydrophilicity. Nonetheless, the study used pectin as a reinforcing agent in chitosan based film; hence, the increase in hydrophilicity would be resulted from the addition of a more hydrophilic polymer. In contrast, coffee pulp film utilized chitosan as a reinforcing agent in a CMC based film; as a result, the less hydrophilicity of chitosan would decrease overall wettability of the coffee pulp film with polyelectrolyte complex structure. The result could also be explained by the roughness of polyelectrolyte complex film (Figure 4.15). The roughening of the film surface would decrease wettability of the film containing hydrophobic polymer (Uelzen and Müller, 2003).

Table 4.8 Comparison between coffee pulp film with and without polyelectrolyte complex structure

Film	Film formulation	
	CM (Formulation 1)	CC (Optimum formulation)
Elongation* (%)	130.33 ± 4.39	55.74 ± 3.80
Tensile Strength* (MPa)	0.3214 ± 0.0780	0.7474 ± 0.0700
WVT* ($g.h^{-1}.m^{2}$)	0.9030 ± 0.0210	0.5694 ± 0.0180
Moisture content (%)	16.95^{b} ± 0.85	20.14^{a} ± 1.06
Solubility (%)	100^{a} ± 0.00	75.75^{b} ± 0.41
Contact angle (°)	42.41^{b} ± 4.50	46.51^{a} ± 7.60

* Predicted values

a,b Different superscripts in the same row means the values are statistically different

DSC thermograms (Figure 4.13) show similar trend for both films with the melting point of CMC approximately at 180°C (Ghanbarzadeh and Almasi, 2011). The appearances of random peaks before the melting of CMC in both treatments indicated possible artifacts formed during testing. Those artifacts might come from an abrupt changes of heat transfer between the film samples and the pans that caused by the films changing shape on initial warming. The statistically equal peak temperature and enthalpy (ΔE) suggested that the polyelectrolyte complex structure had no significant effect on thermal property of the film. The reason that polyelectrolyte complex had no effect on the film thermal properties might be that only small amount complexes were formed on top of the existing network of CMC. Thus, their formation showed negligible effect on the intermolecular force between CMC molecules. The formation of the complex is illustrated in Figure 4.16.

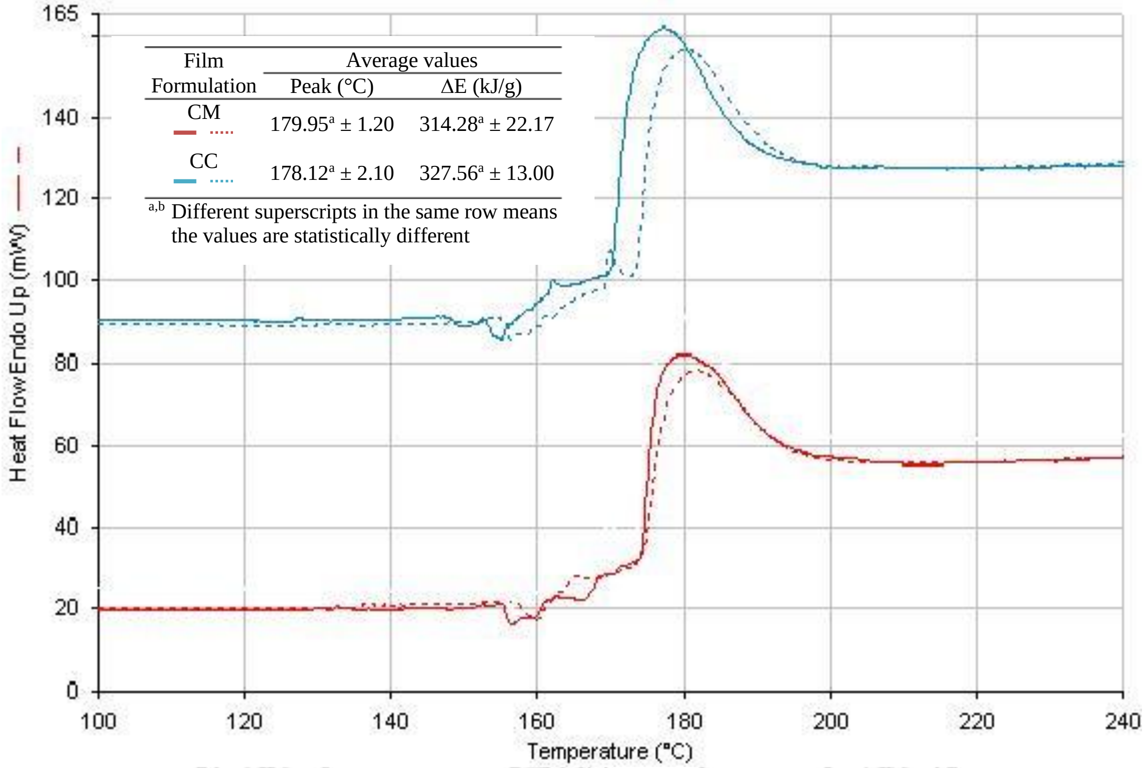

Figure 4.13 DSC thermograms of coffee pulps films

Scanning electron microscope (SEM) was used to study film morphology of the coffee pulp film. Morphologies of film surface and cross-sectioned area of two different film structures were recorded. The morphology of the coffee pulp film without polyelectrolyte complex structure is shown in Figure 4.14; while, Figure 4.16 shows morphologies of the film containing polyelectrolyte complex structure (both surface and cross-sectioned areas). Apart from the impurities that might deposited during the drying or SEM sample preparation processes, overall morphology of the film without polyelectrolyte complex structure showed the homogeneous film structure throughout the film. On the other hand, the film with polyelectrolyte complex structure showed the rough surface that probably comprised of polyelectrolyte complex structure. Surface roughness was also observed in the polyelectrolyte complex film based on gelatin and pectin (Jo *et al.*, 2005). In addition, cross-sectioned area of the film showed a distribution of small particles (1-2 microns in size) throughout the film structure. These particles could also be the polyelectrolyte complex structure that reinforced the film. According to SEM micrographs, thickness of the film with polyelectrolyte complex structure was smaller than CMC film. Therefore, the formation of complex resulted in denser film structure, which more effectively impeded the water molecules from passing despite the more hydrophilic nature of the film.

Figure 4.17 shows almost identical FT-IR spectrums for both film structures. Most of the functional groups in the spectrums came from CMC with characteristic absorption band at 3273-3282 and 2930 cm^{-1} (Su *et al.*, 2010). Absorption band representing phenolic compounds like chlorogenic acid also observed at 1261-1265 cm^{-1} (Lozano-Vazquez *et al.*). Furthermore, the blue shift of hydroxyl group (3273 to 3282 cm^{-1}) and carbonyl group (1590 to 1591 cm^{-1}) in the spectrum of film with polyelectrolyte complex structure, comparing with the film without the complex, might due to the strong ionic interaction from the structure that disrupted hydrogen bonding and impeded the movement of those functional groups resulting in the absorption in the higher wavenumber (Chen *et al.*, 2010). Thus, the evidence to polyelectrolyte complex structure in the film could also be shown by FT-IR spectrum of the film. The lack of characteristic absorption band of chitosan might due to the limitation of the color film that can only be tested using ATR mode, which can only examine the first few microns the film thickness. Therefore, the test area might not thick enough to get through the CMC matrix.

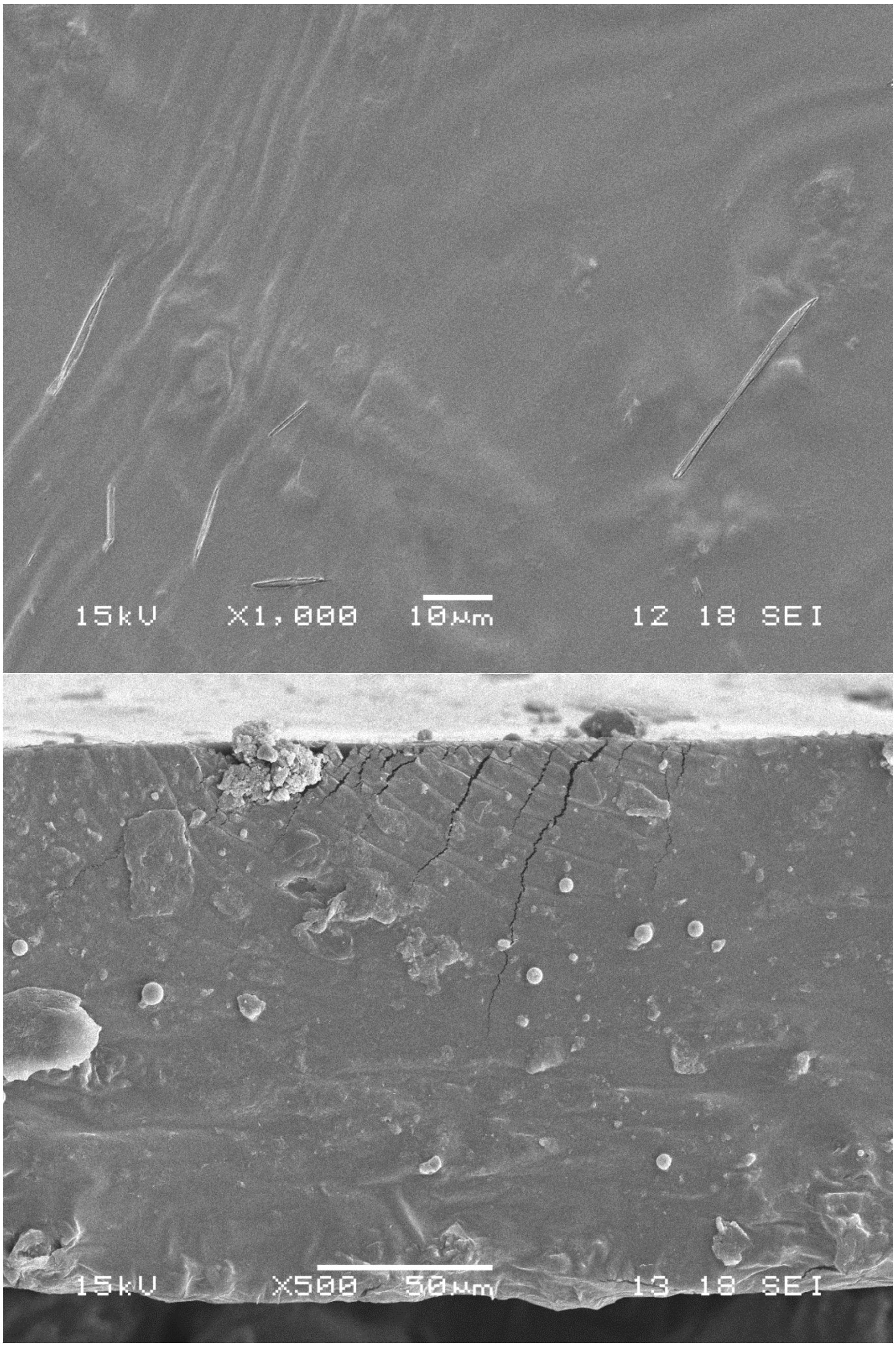

Figure 4.14 SEM micrographs of coffee pulp film without polyelectrolyte complex structure: Surface (top); Cross-section (bottom)

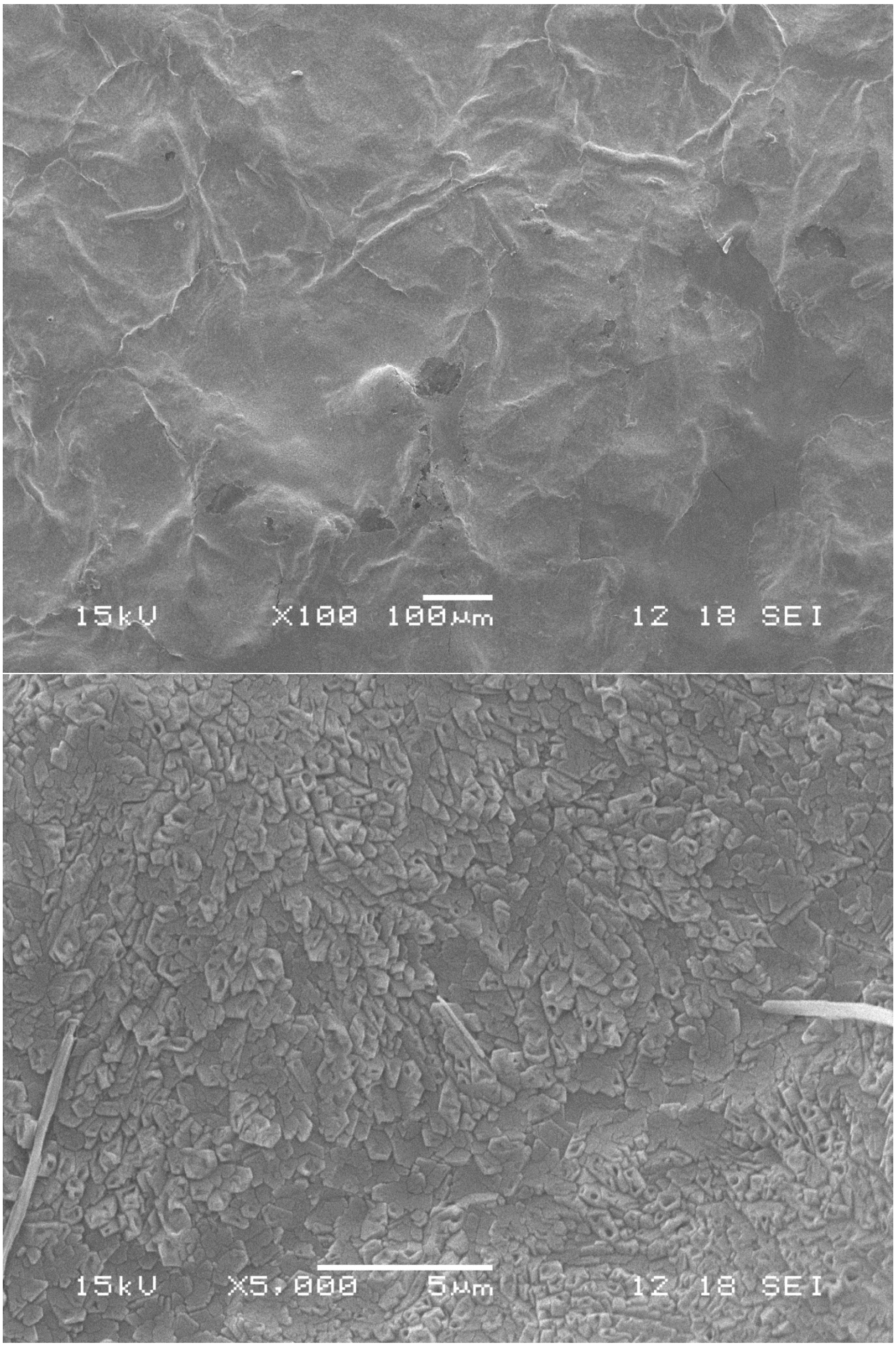

Figure 4.15 SEM micrographs of coffee pulp film surface with polyelectrolyte complex structure: 100x (top); 5,000x (bottom)

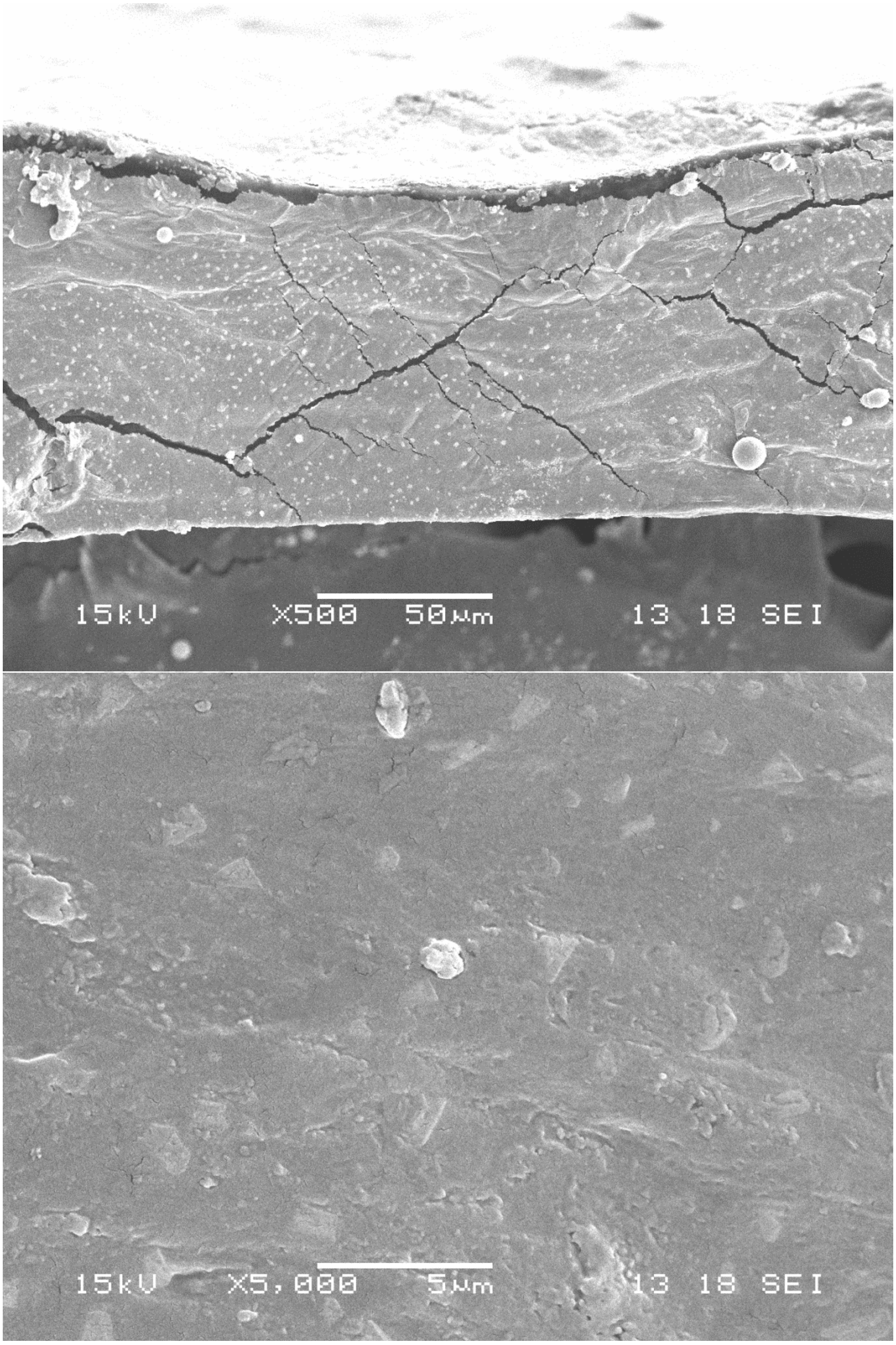

Figure 4.16 SEM micrographs of coffee pulp film crossed-sectioned with polyelectrolyte complex structure: 500x (top); 5,000x (bottom)

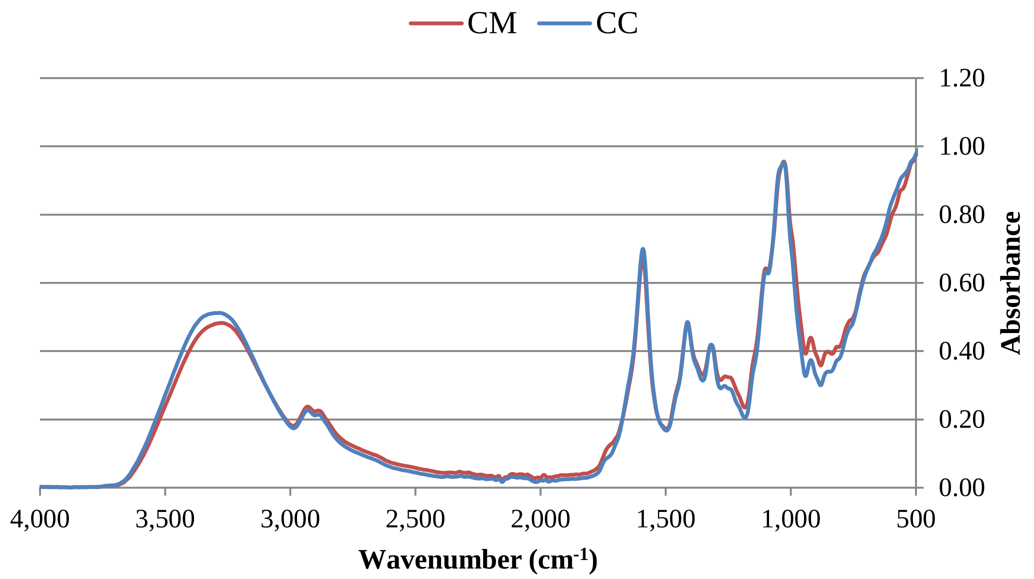

Functional group		Alcohol	Aliphatic	Carboxylic acid	Phenol	Secondary alcohol	Primary alcohol
		-OH stretching	$-CH_2$ stretching	COO^-	-C-O stretching	-C-O stretching	-C-O stretching
Wavenumber (cm^{-1})	CM	3273	2930	1590	1261	1100	1028
	CC	3282	2930	1591	1265	1100	1028

Figure 4.17 FT-IR spectrums of coffee pulp bioplastic

Although polyelectrolyte complex film showed an improvement in overall performance comparing to single polymer film, it still had the same water-sensitivity limitations; for instance, the film under humid conditions would show a reduction in both stiffness and toughness, and the film disintegrated in water over time.

4.5 Coffee Pulp Bioplastic Active Properties

4.5.1 Antioxidant activity

Coffee pulp bioplastic containing chlorogenic acids and other phenolic compounds was verified for it proclaimed antioxidant activity by using DPPH radical scavenging assay. The result concluded that coffee pulp bioplastic had antioxidant activity equivalent to 24.80 ± 1.14 mg of gallic acid per gram of the plastic or with the EC_{50} value of 82.36 ± 3.81 µg/mL. The coffee pulp film showed comparable antioxidant activity to antioxidant film based on catechins and methyl cellulose; EC_{50} 33.8-66.3 μg/mL (Yu *et al.*, 2015), which effectively prevented the degradation of β-carotene from the oxidation process. Thus, coffee pulp film could provide enough antioxidant power to prevent food from oxidation process as well.

4.5.2 Antimicrobial activity

The film from coffee pulp was tested against *Staphylococcus aureus* (gram positive bacteria), *Escherichia coli* (gram negative bacteria) and *Aspergillus niger* (filamentous fungi) as model microorganisms. The antimicrobial test was performed using agar disk diffusion method. The result (Figure 4.18) showed that coffee pulp bioplastic could inhibit the growth of gram positive bacteria (*S. aureus*); while gram negative bacteria and filamentous fungi remained active.

According to Zhao *et al.* (2010), a disk containing 1 μg of chlorogenic acid could effectively inhibit the growth of both *Staphylococcus aureus* and *Escherichia coli* with the inhibition zone greater than 8 mm. Though, the content of chlorogenic acid in the coffee pulp film used in the testing was as high as 120 μg (calculated from the amount of coffee pulp extract in the disk), the poor antimicrobial activity was resulted. Since the film was naturally dried in air conditioned environment, the poor antimicrobial activity might come from the degradation of chlorogenic acid during the drying process and storage. However, the remaining chlorogenic acid content could still inhibit the growth of *Staphylococcus aureus*. This might also contribute to the membrane structure of gram positive bacteria that allowed easy access route of chlorogenic acid to the cell even in a small concentration (Lou *et al.*, 2011). Hence, the antimicrobial testing might indicate a major degradation of chlorogenic acids during film production, which required further study in chlorogenic acid stability to further improve the film activity.

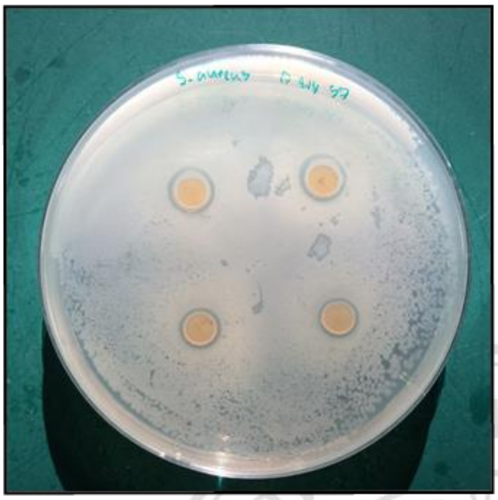	***S. aureus*** Inhibition zone (mm) 1.08 ± 0.08
	***E. coli*** Inhibition zone (mm) Not detect
	***A. niger*** Inhibition zone (mm) Not detect

Figure 4.18 Antimicrobial property of coffee pulp bioplastic

4.5.3 Biodegradability

Biodegradability testing of bioplastic from coffee pulp followed ISO 20200: "Plastics - Determination of the degree of disintegration of plastic materials under simulated composting condition in a laboratory-scale test" (International Standard Organization, 2004). Coffee pulp bioplastic was compared with commercial biodegradable product (Gracz™). The test was performed by putting the film in a natural composting environment, which compost composition was summarized in Table 8, for 30 days. After the test period the test specimens were recovered and calculated for degree of disintegration. The result (Table 4.9) showed that coffee pulp bioplastic could be degraded in natural composting environment better than the commercial product. The superior degradability would come from the water sensitivity of the film that can partially be dissolved in water.

Table 4.9 Biodegradability of coffee pulp bioplastic

Sample	Degree of disintegration (%)
Coffee pulp film	$99.14^{a} \pm 1.49$
Control (GRAC™)	$71.99^{b} \pm 6.69$

^{a,b} Different superscripts in the same column means the values are statistically different

4.5.4 Application testing: shelf life extension of fresh cut carrot

Table 4.10 shows weight loss and microbial load of carrot samples wrapped with coffee pulp film and conventional packaging during 8 days of storage. While, Table 4.11 shows the L*a*b* color value of the samples.

Table 4.10 Weight loss and total plate count of fresh cut carrot with different packaging during 8 days of storage

Day	Weight loss (%)		Total plate count (log CFU/g)	
	Control	Coffee pulp film	Control	Coffee pulp film
0	0		3.627 ± 0.088	
2	1.04^{b} ± 0.57	32.34^{a} ± 6.88	7.128^{a} ± 0.081	7.300^{a} ± 0.177
4	1.60^{b} ± 0.30	48.72^{a} ± 1.46	7.491^{b} ± 0.391	8.473^{a} ± 0.068
6	2.23^{b} ± 0.19	52.71^{a} ± 3.17	8.121^{b} ± 0.099	8.717^{a} ± 0.268
8	2.65^{b} ± 0.59	61.69^{a} ± 2.47	8.044^{b} ± 0.080	8.871^{a} ± 0.096

^{a,b} Different superscripts in the same row means the values are statistically different

Table 4.11 Color (L*a*b*) of fresh cut carrot with different packaging during 8 days of storage

Day	Color					
	L*		a*		b*	
	Control	Sample	Control	Sample	Control	Sample
0	56.49 ± 01.87		35.69 ± 00.62		75.75 ± 01.91	
2	57.54^{a} ± 3.08	51.03^{b} ± 0.10	32.65^{b} ± 0.12	38.09^{a} ± 2.90	70.01^{b} ± 0.25	73.58^{a} ± 2.76
4	52.81^{a} ± 1.39	54.28^{a} ± 1.75	28.60^{b} ± 1.35	31.66^{a} ± 1.02	49.32^{a} ± 1.63	50.81^{a} ± 0.38
6	55.10^{a} ± 0.97	52.27^{b} ± 0.74	25.32^{a} ± 0.22	26.95^{a} ± 2.60	47.30^{a} ± 1.35	44.10^{a} ± 2.70
8	50.62^{a} ± 1.18	44.64^{b} ± 1.50	24.37^{a} ± 2.39	25.22^{a} ± 0.12	43.18^{a} ± 2.20	39.82^{b} ± 1.16

^{a,b} Different superscripts in the same row means the values are statistically different

During the 8 days storage period, carrots wrapped with coffee pulp showed weight loss excessively greater than conventional packaging. The weight loss of carrot wrapped with coffee pulp film was more than 60% when stored at 10°C for 8 days. When compared to a less than 3% weight loss from the sample wrapped polyvinylchloride cling film, coffee pulp film performed very poor in retaining water from the carrot samples. However, the loss of moister more than 30 grams from approximately 72.25 cm^2 film surface was too high comparing to the value (approximately 0.8 g) calculated from WVT of coffee pulp film. This substantial difference might come from the hydrogel structure of coffee pulp film that was very hydrophilic and could retain high amount of water (Chang and Lin, 2000; Chen *et al.*, 2010). Thus, when in close contact of high water content material such as fresh cut carrot, the water in carrot would be transferred to the film until equilibrium had reached. The slower weight loss shown in Figure 4.19 indicates water absorption to the film was close to equilibrium when the shelf life approaching 8th day. Moreover, when coupled with the damage from fresh cut process to the carrot integrity and the evaporation of water from the film surface during the storage, the severe weight loss of the samples wrapped with coffee pulp film was highly enhanced.

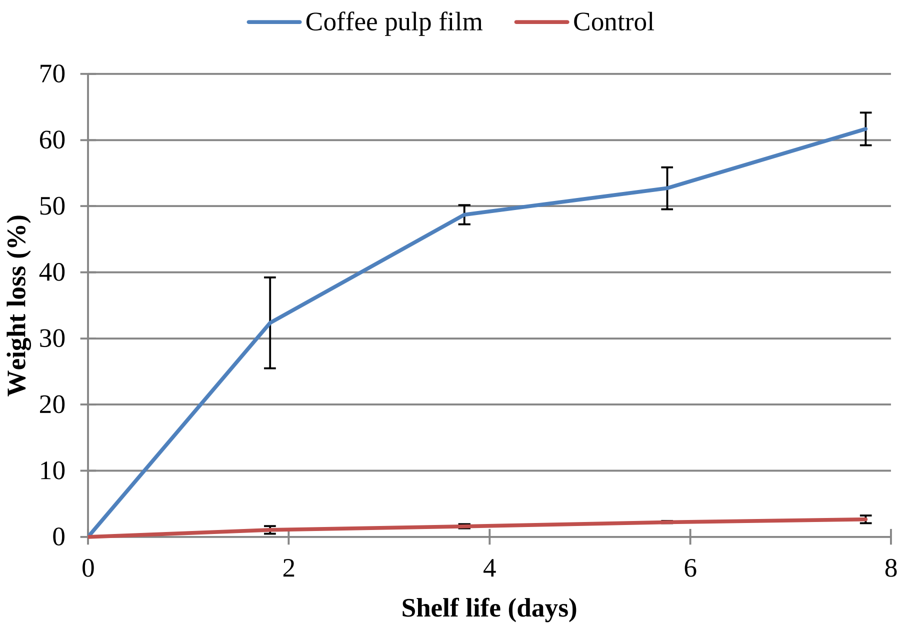

Figure 4.19 Change in weight loss of fresh cut carrot with different packaging during 8 days of storage

Microbial load of carrot samples packed in both packaging systems showed similar trend of microbial growth. Figure 4.20 depicts the log phase of microbial growth during the first 2 days of storage and stationary phase of microbial growth when approaching the last day of the storage. During the log phase both packaging system had statistically equivalent microbial load. This indicated that slight antimicrobial activity of coffee pulp was ineffective in slowing down the growth of the microbes in fresh cut carrot. Moreover, when approaching a stationary phase of the microbial growth, the carrot sample wrapped with coffee pulp film showed higher microbial load than the conventional packaging system. The reason behind this might be that the gas barrier of synthetic polymer (polyvinyl cling film) was higher than natural derived polymer (coffee pulp film)

(Espinel Villacrés *et al.*, 2014; Muppalla *et al.*, 2014); thus, as time passed, the atmosphere in the control packaging would have changed to be less in O_2 and more in CO_2, which was unfavorable for the growth of microbes (Mastromatteo *et al.*, 2012). Consequently, at the latter day of storage, microbial load in the carrot samples wrapped with polyvinyl chloride cling film was less than the samples wrapped with coffee pulp film, which allowed more favorable atmosphere for the growth of microbes.

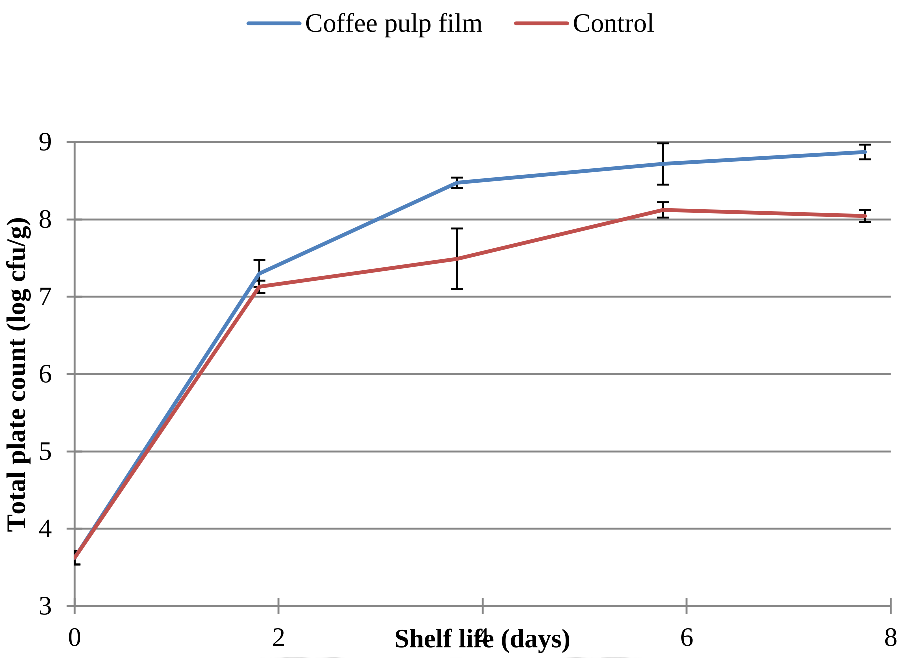

Figure 4.20 Change in microbial load (total plate count) of fresh cut carrot with different packaging during 8 days of storage

Change in color reflects the browning progress of fresh cut carrot. The color change involves the loss of bright orange color and can be monitored according to the color parameters (L* a* b*). During the progress of browning of carrot, the carrot color was turning from bright orange color into the brownish color which reflected by a reduction of all color parameters. Figure 4.21 shows the change of color parameters of fresh cut carrot with different packaging during 8 days of storage. Brightness (L*) of fresh cut carrot was reduced as the shelf life increased for both packaging. Fresh cut carrot wrapped by coffee pulp film loose its brightness faster than the sample with conventional packaging. Usually the loss of brightness of carrot is governed by two processes, loss of water and browning process (Mastromatteo *et al.*, 2012). Thus, the faster loss in brightness in the samples with coffee pulp film was caused by either the two processes was more intense. But, the higher weight loss from samples wrapped by coffee pulp film suggested that loss of moisture from the samples was the major cause of the loss in brightness.

Though the brightness of the carrot wrapped with coffee pulp film reduced faster than that of wrapped by polyvinyl chloride cling film, its orange color was initially faded slower. The change could be seen in Table 4.11 and Figure 4.21 that both a* (redness) and b* (yellowness) in samples wrapped by coffee pulp film were statistically higher than the control. In the case of coffee pulp film, the change in color might be slowed down by antioxidant activity of the film. The antioxidant can prevent the degradation of β-carotene which is a major carrot pigment (Yu *et al.*, 2015). However, the sample wrapped with coffee pulp film had a severe moisture loss. The loss of moisture might increase the concentration of color pigments; thus, the color in the sample would be more saturated than the control sample that had only a minor moisture loss. Therefore, the effectiveness of coffee pulp film in preventing the loss of color from fresh cut carrot was still uncertain without further investigation on the actual amount of color pigments. Furthermore, b* value of carrot wrapped by coffee pulp film was lower than the control when the samples were kept for 8 days. This change might indicate that antioxidant activity of coffee pulp film was only lasted for two days. As a result, the fading of orange color of fresh cut carrot was slower in the carrot wrapped polyvinyl chloride cling film as O_2 molecules responsible for browning process might be better prevented from entering. This was because the presence of polyelectrolyte complex structure as well as impurities from crude coffee pulp extract created extra spaces in the film structure allowing more gasses to pass through. Moreover, a gas barrier of synthetic polymer is usually higher than natural derived polymer (Espinel Villacrés *et al.*, 2014; Muppalla *et al.*, 2014).

According to the microbiological criteria, the shelf life of fresh cut carrot wrapped with coffee pulp film was 2 days which was less than conventional packaging system (polyvinyl chloride cling film), which was 4 days.

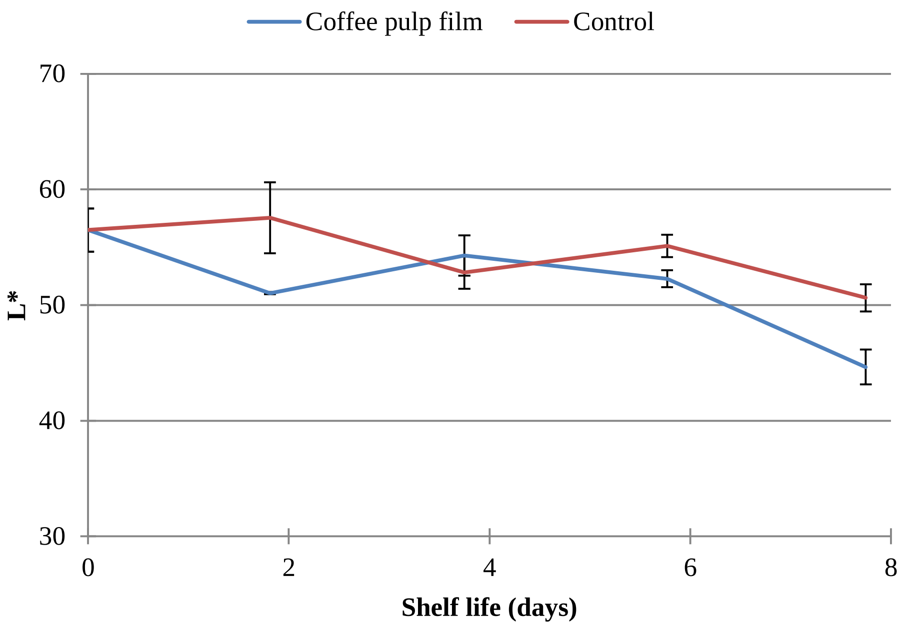

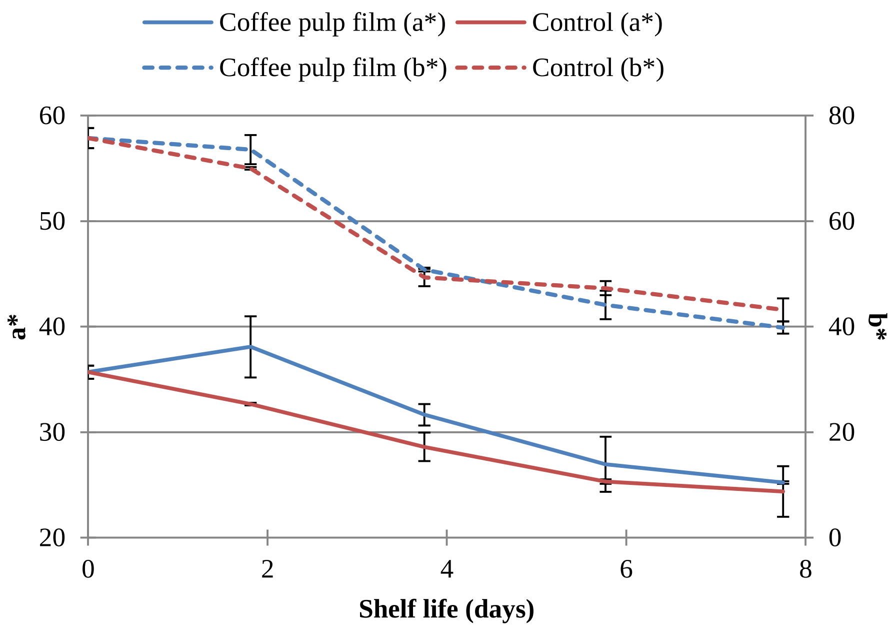

Figure 4.21 Change in color of fresh cut carrot with different packaging during 8 days of storage: L* (top); a* and b* (bottom)

4.6 Production Cost

Table 4.12 Production cost of a 14 x 22 cm^2 sheet of coffee pulp film (4.99 ± 0.15 g)

Material	Amount	unit	Price/unit (Baht)	Production Cost (Baht)
Fresh coffee pulp	65.07	g	0	0
Hydrochloric acid (32%)	0.47	g	0.0032	0.0015
Sodium hydroxide	1.56	g	0.0096	0.015
Sodium silicate	0.46	g	0.0074	0.0034
Hydrogen peroxide (30%)	15.19	g	0.0096	0.1458
Chloroacetic acid	2.31	g	0.024	0.0555
Isopropanol	45.45	g	0.032	1.4545
Ethanol	63.37	g	0.0058	0.365
Methanol	43.24	g	0.0128	0.5535
Chitosan	0.45	g	2.5	1.125
Glycerol	0.72	g	0.032	0.023
Sodium chloride	0.6	g	0.0032	0.0019
Acetic acid	0.6	g	0.016	0.0096
Water	427.63	mL	0.01	4.2763
Electricity	1.16	Unit	2.6506	3.0684
Total				11.0984